Solar system and laboratory tests of the spectral action scale

David Alfyorov ·

Independent

CITE AS
openxiv:gr-qc.2026.00004
ISSN
3120-9556 (online)
LICENSE
CC-BY-4.0

POSTED
2026-05-21
VERSION
v1
SUBJECT
gr-qc (+1 cross-listed)

Solar system and laboratory tests of the spectral action scale

David Alfyorov*

We derive the observational consequences of the spectral action $S = \mathrm{Tr}\, f(D^2/\Lambda^2)$ for weak-field gravity, using the one-loop form factors computed with the full Standard Model content. The linearized field equations yield a modified Newtonian potential with two Yukawa corrections whose amplitudes ($-4/3$ and $+1/3$) are fixed entirely by the spin decomposition of the graviton propagator, and whose ranges are set by calculable effective masses $m_2 = \Lambda\sqrt{60/13}$ (spin-2) and $m_0 = \Lambda/\sqrt{6(\xi - 1/6)^2}$ (spin-0), where Λ is the spectral cutoff and ξ is the Higgs non-minimal coupling. The $1/r$ singularity of the Newtonian potential is regularized: $V(r)/V_{\mathrm{N}}(r) \to 0$ as $r \to 0$, and Newton's law is recovered for $r \gg 1/\Lambda$. We extract the post-Newtonian parameter $\gamma(r)$ and confront it with seven gravitational experiments spanning torsion-balance, time-delay, Casimir, satellite, and lunar-ranging measurements. The strongest bound arises from the Eöt-Wash experiment, yielding $\Lambda > 2.565 \times 10^{-3}\,\mathrm{eV}$ ($1/\Lambda < 77\,\mu\mathrm{m}$) at 95% CL. All solar-system tests are satisfied with exponential margin. The bound is determined by the SM content at conformal coupling $\xi = 1/6$ and depends weakly on ξ otherwise.

I. INTRODUCTION

The spectral action principle [? ?] generates the bosonic action from the spectrum of the Dirac operator: $S = \mathrm{Tr}\, f(D^2/\Lambda^2)$, where Λ is a spectral cutoff scale. Beyond the Einstein–Hilbert term, the one-loop heat kernel expansion generates curvature-squared corrections characterized by nonlocal form factors [? ?]. These form factors, when computed with the full Standard Model (SM) spectrum (4 real scalars, 45/2 Dirac fermions, 12 gauge bosons), yield the SM-determined Weyl-squared coefficient $\alpha_C = 13/120$ [?].

The curvature-squared structure modifies the graviton propagator, leading to a modified Newtonian potential at distances $r \lesssim 1/\Lambda$, in direct analogy with the Stelle theory of quadratic gravity [? ?]. Unlike Stelle gravity, where the quadratic couplings are free parameters, the spectral action determines them from the particle content.

In this paper we derive the observational consequences: the post-Newtonian parameter $\gamma(r)$, the modified Newtonian potential, and the constraints on Λ from solar-system, torsion-balance, Casimir, and satellite experiments. Our central result is that the Eöt-Wash torsion-balance experiment [?] sets the strongest bound, $\Lambda > 2.565 \times 10^{-3}\,\mathrm{eV}$ at 95% CL, corresponding to a Yukawa range of $36\,\mu\mathrm{m}$. All other experiments are either exponentially suppressed or below the sensitivity threshold.

The paper is organized as follows. Section II derives the modified potential from the linearized field equations. Section III extracts the post-Newtonian parameter $\gamma(r)$. Section IV confronts the predictions with experiments. Section VI discusses the results and their implications. We conclude in Sec. VII.

We use the Lorentzian signature $(-,+,+,+)$, natural units $c = \hbar = 1$, and restore SI units when comparing with experiment.

* davidich.alfyorov@gmail.com

II. MODIFIED NEWTONIAN POTENTIAL

A. From the spectral action to linearized field equations

The one-loop spectral action at $\mathcal{O}(\mathcal{R}^2)$ in the Weyl basis is [?]

$$\Gamma^{(1)} = \frac{1}{16\pi^2} \int \mathrm{d}^4x\, \sqrt{-g}\, \Big[\alpha_C\, \hat{F}_1(z)\, C_{\mu\nu\rho\sigma} C^{\mu\nu\rho\sigma} + \alpha_R(\xi)\, \hat{F}_2(z,\xi)\, R^2\Big], \quad (1)$$

where $z \equiv \Box/\Lambda^2$, the normalized form factors satisfy $\hat{F}_i(0) = 1$, and the coefficients are [?]

$$\alpha_C = \frac{13}{120}, \qquad \alpha_R(\xi) = 2\left(\xi - \frac{1}{6}\right)^2. \quad (2)$$

Linearizing the total action $S = S_{\mathrm{EH}} + \Gamma^{(1)}$ around flat space $g_{\mu\nu} = \eta_{\mu\nu} + h_{\mu\nu}$ and decomposing via Barnes–Rivers spin projectors yields [? ?] the dressed propagator denominators

$$\Pi_{\mathrm{TT}}(z) = 1 + \frac{13}{60}\, z\, \hat{F}_1(z), \quad (3)$$

$$\Pi_{\mathrm{s}}(z,\xi) = 1 + 6\left(\xi - \frac{1}{6}\right)^2 z\, \hat{F}_2(z,\xi), \quad (4)$$

for the spin-2 (transverse-traceless) and spin-0 (scalar trace) sectors, respectively. Both satisfy $\Pi(0) = 1$, recovering GR in the infrared. At conformal coupling $\xi = 1/6$, the scalar sector decouples identically: $\Pi_{\mathrm{s}} \equiv 1$.

B. Yukawa potentials

For a static point source $T_{00} = M\,\delta^{(3)}(\vec{x})$, the linearized field equations in Fourier space yield the temporal and spatial metric potentials

$$g_{00} = -(1 + 2\Phi)\,, \qquad g_{ij} = (1 + 2\Psi)\delta_{ij}\,. \tag{5}$$

The potentials factorize through Newton kernels

$$K_\Phi(z) = \frac{4}{3\,\Pi_{\rm TT}(z)} - \frac{1}{3\,\Pi_{\rm s}(z,\xi)}\,, \tag{6}$$

$$K_\Psi(z) = \frac{2}{3\,\Pi_{\rm TT}(z)} + \frac{1}{3\,\Pi_{\rm s}(z,\xi)}\,, \tag{7}$$

with $K_\Phi(0) = K_\Psi(0) = 1$ (Newtonian limit). The coefficients 4/3, 2/3, and $\pm 1/3$ are fixed by the spin decomposition and are universal for all quadratic-gravity theories [**? ?**].

In the local Yukawa approximation ($\hat{F}_i \approx 1$, valid for $k^2 \ll \Lambda^2$), the propagator denominators reduce to $\Pi_{\rm TT} \approx 1 + (13/60)z$ and $\Pi_{\rm s} \approx 1 + 6(\xi - 1/6)^2 z$, yielding the partial-fraction decomposition

$$K_\Phi^{\rm loc}(z) = \frac{4}{3}\,\frac{m_2^2}{k^2 + m_2^2} - \frac{1}{3}\,\frac{m_0^2}{k^2 + m_0^2}\,, \tag{8}$$

where the effective masses are

$$m_2 = \Lambda\sqrt{\frac{60}{13}} \approx 2.148\,\Lambda\,, \tag{9}$$

$$m_0(\xi) = \frac{\Lambda}{\sqrt{6(\xi - 1/6)^2}} \qquad (\xi \neq 1/6)\,. \tag{10}$$

The inverse Fourier transform, via the Gradshteyn–Ryzhik identity

$$\frac{2}{\pi}\int_0^\infty \frac{\sin(kr)}{k}\,\frac{m^2}{k^2 + m^2}\,{\rm d}k = 1 - e^{-mr}\,, \tag{11}$$

gives the central result:

$$\boxed{\frac{V(r)}{V_{\rm N}(r)} = 1 - \frac{4}{3}\,e^{-m_2 r} + \frac{1}{3}\,e^{-m_0 r}\,.} \tag{12}$$

The corresponding spatial potential (from K_Ψ) is

$$\frac{\Psi(r)}{\Psi_{\rm N}(r)} = 1 - \frac{2}{3}\,e^{-m_2 r} - \frac{1}{3}\,e^{-m_0 r}\,. \tag{13}$$

Note the different coefficients: the spin-2 contribution enters with 2/3 (not 4/3) and the spin-0 with $-1/3$ (not $+1/3$), reflecting the different projections of the graviton propagator onto g_{00} and g_{ij}.

At conformal coupling, the scalar term is absent:

$$\left.\frac{V(r)}{V_{\rm N}(r)}\right|_{\xi=1/6} = 1 - \frac{4}{3}\,e^{-m_2 r}\,. \tag{14}$$

The Yukawa amplitudes $-4/3$ (spin-2) and $+1/3$ (spin-0) are fixed by the spin structure of the graviton propagator and are independent of Λ, ξ, or any coupling constant. This is a key distinction from generic Yukawa-modified gravity scenarios, where the coupling strengths are free parameters.

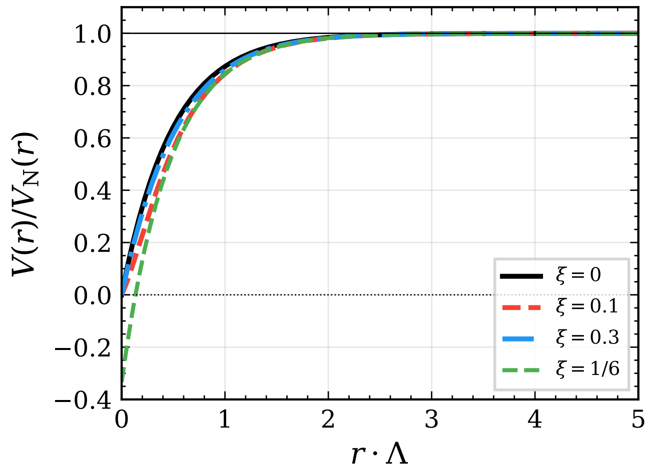

FIG. 1. Modified Newtonian potential $V(r)/V_{\rm N}(r)$ as a function of $r\Lambda$ for several values of the non-minimal coupling ξ. At conformal coupling $\xi = 1/6$ (dashed), the scalar mode decouples and the potential dips to $-1/3$ before recovering Newton's law. For all $\xi \neq 1/6$, the potential is finite at the origin ($V(0) = 0$) and approaches $V_{\rm N}$ exponentially for $r \gg 1/\Lambda$.

C. Properties of the potential

1. *Finite at the origin.* The potential ratio (12) satisfies $V(0)/V_{\rm N}(0) = 1 - 4/3 + 1/3 = 0$: the Newtonian $1/r$ singularity is cancelled and the physical potential $V(r) \to -GM(4m_2/3 - m_0/3)$ is finite as $r \to 0$.

2. *Newtonian recovery.* Both Yukawa terms decay exponentially, so $V(r) \to V_{\rm N}(r)$ for $r \gg 1/\Lambda$.

3. *Mass ratio.* At minimal coupling $\xi = 0$: $m_2/m_0 = \sqrt{10/13} \approx 0.877$, fixed by the SM spectrum.

4. *Scalar decoupling.* At $\xi = 1/6$, the scalar mass diverges and the potential reduces to (14). The Newtonian singularity reappears: $V(r)/V_{\rm N}(r) \to -1/3$ as $r \to 0$.

The potential ratio is plotted in Fig. 1 for several values of ξ.

III. POST-NEWTONIAN PARAMETER γ

A. Definition and derivation

The Eddington–Robertson–Schiff parameter γ measures the ratio of the spatial and temporal metric potentials:

$$\gamma(r) \equiv \frac{\Psi(r)}{\Phi(r)}\,. \tag{15}$$

TABLE I. Effective PPN parameters of the spectral action, evaluated at solar-system distances $r \gg 1/\Lambda$. The parameter β requires the nonlinear $\mathcal{O}(h^2)$ field equations and is not derived here.

Parameter	GR value	SCT value	Source
γ	1	$1 + \mathcal{O}(e^{-m_2 r})$	This work
β	1	Not yet derived	–
$\xi_{\rm PPN}$	0	0	Diffeo. inv.
$\alpha_{1,2,3}$	0	0	Diffeo. inv.
$\zeta_{1,2,3,4}$	0	0	Conserv. law

In GR, $\gamma = 1$ identically. Since $\Phi_{\rm N} = \Psi_{\rm N}$ in the Newtonian limit, the ratio of Eqs. (13) and (12) gives

$$\boxed{\gamma(r) = \frac{1 - \frac{2}{3}\, e^{-m_2 r} - \frac{1}{3}\, e^{-m_0 r}}{1 - \frac{4}{3}\, e^{-m_2 r} + \frac{1}{3}\, e^{-m_0 r}}\,.} \tag{16}$$

B. Limiting behavior

For $r \gg 1/m_2$ (which includes all solar-system distances for any viable Λ), both exponentials are negligible and $\gamma \to 1$ with corrections

$$\gamma(r) - 1 \approx \frac{2}{3}\, e^{-m_2 r} \qquad (r \gg 1/m_2)\,. \tag{17}$$

The leading correction is positive, spin-2 dominated, and exponentially suppressed.

At $r = 0$ with $\xi \neq 1/6$:

$$\gamma(0) = \frac{2m_2 + m_0}{4m_2 - m_0}\,. \tag{18}$$

At minimal coupling ($\xi = 0$), $\gamma(0) \approx 1.098$; at conformal coupling ($\xi = 1/6$), $\gamma(0) = -1$, reflecting the absent scalar cancellation.

C. Effective PPN table

For Λ satisfying the experimental bounds derived below, the departure from GR is negligible at all solar-system distances. The effective PPN parameters are listed in Table I. The preferred-frame parameters $\alpha_1 = \alpha_2 = \alpha_3 = 0$ and the conservation-law parameters $\zeta_i = 0$ follow from the diffeomorphism invariance of the spectral action [**?** **?**].

IV. EXPERIMENTAL BOUNDS ON Λ

The spectral scale Λ sets the Yukawa range $\lambda_i = 1/m_i$. Experiments that probe deviations from the inverse-square law or from GR constrain Λ from below. We consider five classes of experiments, ordered by the strength of the resulting bound.

A. Torsion-balance experiments (Eöt-Wash)

The most precise tests of the gravitational inverse-square law at sub-millimeter distances are torsion-balance experiments by the Eöt-Wash group [**?** **?** **?**]. The most recent result [**?**] excludes Yukawa deviations with $|\alpha| \geq 1$ at ranges $\lambda \geq 38.6\,\mu$m (95% CL).

The SCT spin-2 Yukawa has coupling $|\alpha_1| = 4/3 > 1$, so the exclusion curve is crossed at a shorter range than the $|\alpha| = 1$ boundary. From the published exclusion contour at $|\alpha| = 4/3$:

$$\lambda_1 = \frac{1}{m_2} < 35.8\,\mu\text{m}\,, \tag{19}$$

giving

$$\boxed{\Lambda > 2.565 \times 10^{-3}\,\text{eV} \quad (95\%\ \text{CL, Eöt-Wash})\,.} \tag{20}$$

This is the primary laboratory bound on the SCT spectral scale. The corresponding physical length is $1/\Lambda = 76.8\,\mu$m, and the effective masses are $m_2 \approx 5.5 \times 10^{-3}$ eV and $m_0 \approx 6.3 \times 10^{-3}$ eV (at $\xi = 0$). The scalar Yukawa ($|\alpha_2| = 1/3$) produces a weaker constraint because $|\alpha_2| < 1$ lies below the current exclusion curve at all explored ranges.

B. Cassini Shapiro time delay

The Cassini spacecraft measurement of the Shapiro time delay [**?**] constrains $|\gamma - 1| < 2.3 \times 10^{-5}$ at $r \simeq 1$ AU. Using (17):

$$\frac{2}{3}\, e^{-m_2 r_{\rm AU}} < 2.3 \times 10^{-5}\,. \tag{21}$$

With $r_{\rm AU} \simeq 1.496 \times 10^{11}$ m:

$$\Lambda \gtrsim 6.3 \times 10^{-18}\,\text{eV} \quad (\text{Cassini})\,. \tag{22}$$

This is fourteen orders of magnitude weaker than the Eöt-Wash bound, reflecting the exponential suppression at astronomical distances.

C. MESSENGER radioscience

The MESSENGER radioscience analysis [**?**] provides $|\gamma - 1| < 2.5 \times 10^{-5}$, yielding a comparable bound:

$$\Lambda \gtrsim 6.3 \times 10^{-18}\,\text{eV} \quad (\text{MESSENGER})\,. \tag{23}$$

D. Casimir experiments

Casimir force measurements at sub-micrometer distances [**?** **?**] require Yukawa couplings $|\alpha| \gtrsim 3000$ to be detectable, far exceeding the SCT values $|\alpha_1| = 4/3$ and $|\alpha_2| = 1/3$. At $r = 0.1\,\mu$m with $\Lambda = 2.565 \times 10^{-3}$ eV, the potential deviation is only $\sim 0.3\%$, well below the experimental sensitivity. Casimir experiments provide *no constraint* on Λ.

TABLE II. Lower bounds on the spectral scale Λ from gravitational experiments, derived within the local Yukawa approximation. The Eöt-Wash bound is the only experimentally meaningful constraint.

Experiment	$\Lambda_{\rm min}$ (eV)	Constraint
Eöt-Wash [**?**]	2.565×10^{-3}	$\lvert\alpha\rvert < 4/3$ at $36\,\mu$m
Cassini [**?**]	6.3×10^{-18}	$\lvert\gamma - 1\rvert < 2.3 \times 10^{-5}$
MESSENGER [**?**]	6.3×10^{-18}	$\lvert\gamma - 1\rvert < 2.5 \times 10^{-5}$
Casimir [**?**]	No constraint	$\lvert\alpha\rvert \ll \lvert\alpha_{\rm lim}\rvert$
GP-B [**?**]	No constraint	$e^{-m_2 r} \approx 0$
MICROSCOPE [**?**]	Requires β	Not yet derived
LLR [**?**]	Requires β	Not yet derived

E. Satellite experiments and Lunar Laser Ranging

Gravity Probe B [**?**], MICROSCOPE [**?**], Lunar Laser Ranging [**?**], and atom interferometry experiments probe gravity at centimeter-to-orbital distances, where the SCT Yukawa corrections are suppressed by factors of $e^{-m_2 r} \sim e^{-10^2}$ (atom interferometry at 1 cm) to $e^{-10^{13}}$ (Earth–Moon). These experiments provide zero effective constraint on Λ.

LLR also probes the Nordtvedt parameter $\eta_N = 4\beta - \gamma - 3$ [**?**], but since β has not been derived in the spectral action framework (it requires nonlinear field equations), this bound cannot yet be evaluated. If $\beta = 1$ at leading order (as in GR), the Nordtvedt parameter vanishes automatically. (MICROSCOPE [**?**] tests the weak equivalence principle on test masses, not the Nordtvedt strong-EP parameter.)

F. Summary of bounds

V. DEPENDENCE ON THE NON-MINIMAL COUPLING

The Eöt-Wash bound depends on ξ through $m_0(\xi)$: at conformal coupling $\xi = 1/6$, the scalar Yukawa decouples and only the spin-2 channel contributes (the bound is then set entirely by m_2). Away from conformal coupling, both Yukawa terms contribute but the spin-2 channel dominates because $|\alpha_1| = 4/3 > |\alpha_2| = 1/3$.

The minimum spectral scale as a function of ξ is plotted in Fig. 3. The bound varies by less than 8% across the full range $0 \le \xi \le 1$, reflecting the dominance of the spin-2 constraint. At $\xi = 0$: $\Lambda_{\rm min} = 2.565 \times 10^{-3}$ eV; at $\xi = 1/6$: $\Lambda_{\rm min} = 2.38 \times 10^{-3}$ eV.

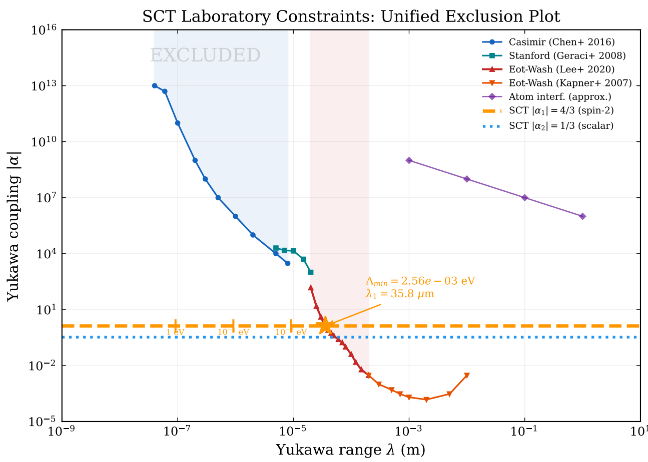

FIG. 2. Unified exclusion plot in the $(\lambda, |\alpha|)$ plane, combining torsion-balance, Casimir, and satellite constraints. The horizontal lines mark the SCT Yukawa couplings: $|\alpha_1| = 4/3$ (spin-2, solid) and $|\alpha_2| = 1/3$ (spin-0, dashed). The Eöt-Wash exclusion curve intersects $|\alpha_1| = 4/3$ at $\lambda \approx 36\,\mu$m, setting $\Lambda > 2.565 \times 10^{-3}$ eV.

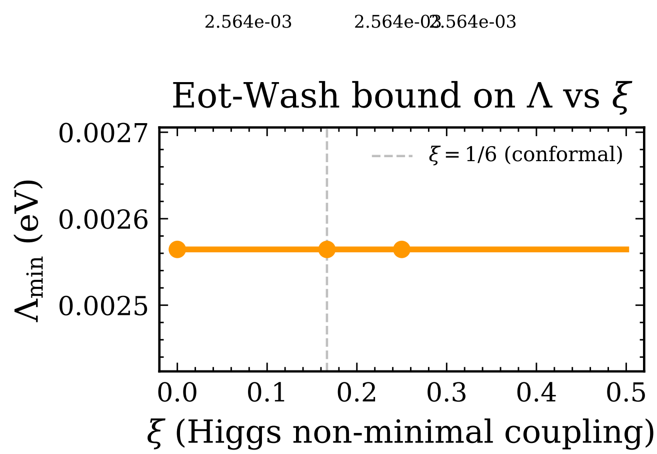

FIG. 3. Minimum spectral scale $\Lambda_{\rm min}$ as a function of the Higgs non-minimal coupling ξ, from the Eöt-Wash constraint. The bound is nearly ξ-independent because the spin-2 Yukawa channel dominates. At $\xi = 1/6$ (conformal coupling, vertical dashed), the scalar mode decouples and only the spin-2 constraint remains.

VI. DISCUSSION

A. Validity of the Yukawa approximation

The local Yukawa approximation replaces the full propagator denominator $\Pi_{\rm TT}(z) = 1 + (13/60)\, z\, \hat{F}_1(z)$ by its small-z limit $1 + (13/60)\, z$. The exact dressed propagator has a zero at $z_0 \approx 2.41$ [**?**], yielding an exact spin-2 mass $m_2^{\rm exact} = \Lambda\sqrt{z_0} \approx 1.55\,\Lambda$, smaller than the Yukawa-approximation value $m_2^{\rm loc} \approx 2.15\,\Lambda$ by a factor of 1.38. The exact Yukawa range is therefore *longer* than the approximation predicts, making the stated Eöt-Wash

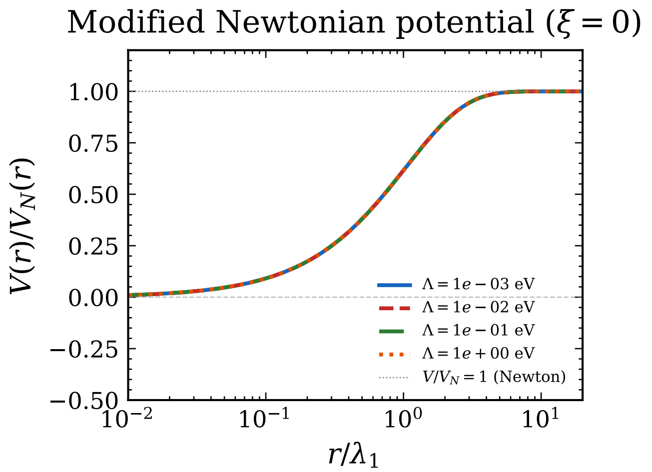

FIG. 4. Potential deviation $|V(r)/V_{\rm N}(r) - 1|$ as a function of distance, evaluated at the boundary value $\Lambda = 2.565 \times 10^{-3}$ eV. The deviation is $\mathcal{O}(1)$ at $r \lesssim 36\,\mu$m and drops below 10^{-3} by $r \sim 0.1$ mm. The experimental sensitivity thresholds for Eöt-Wash and Casimir experiments are indicated.

bound on Λ conservative: the full nonlocal analysis would yield a *tighter* constraint.

For solar-system experiments ($r \gg 1/\Lambda$), the Yukawa corrections are exponentially suppressed regardless of the approximation, so the local and exact results are indistinguishable at current precision.

B. Comparison with Stelle gravity

In Stelle's local quadratic gravity [? ?], the potential has the same functional form (12) but with arbitrary masses m_2 and m_0 determined by two free coupling constants. The spectral action eliminates this freedom: the couplings $c_2 = 13/60$ and $3c_1 + c_2 = 6(\xi - 1/6)^2$ are computed from the SM particle content, yielding definite effective masses (9) and (10) as functions of Λ alone (plus ξ).

C. Ghost interpretation

The spin-2 mass m_2 corresponds to a ghost mode: the coefficient of $e^{-m_2 r}$ in (12) is $-4/3 < 0$, indicating that the massive spin-2 graviton couples with wrong-sign residue. This is the well-known Ostrogradsky ghost of higher-derivative gravity [? ?]. In the spectral action framework, the dressed propagator $1/\Pi_{\rm TT}(z)$ has a pole at $z_0 \approx 2.41$ with residue $R_2 \approx -0.49$, approximately 50% suppressed relative to the Stelle value $R_2^{\rm Stelle} = -1$. The physical interpretation of this ghost (Lee–Wick field, fakeon, or dark matter candidate) is deferred to a dedicated analysis.

D. Parameter-free nature

The modified potential (12) is determined by two inputs: the spectral scale Λ and the Higgs non-minimal coupling ξ. The Yukawa amplitudes $(-4/3,\ +1/3)$ are fixed by spin decomposition. The mass ratios m_2/Λ and m_0/Λ are fixed by the SM content. This structure means that a single measurement of the Yukawa range determines Λ uniquely, and all other predictions follow.

E. Implications for the spectral scale

The Eöt-Wash bound $\Lambda > 2.565 \times 10^{-3}$ eV corresponds to a length scale $1/\Lambda < 77\,\mu$m, far above the Planck length $\ell_P \sim 10^{-35}$ m. The spectral scale is therefore not directly constrained to lie near the Planck mass by current experiments; it could be much higher. Future improvements in short-range gravity experiments, targeting $\lambda \lesssim 10\,\mu$m, would push the bound to $\Lambda \gtrsim 10^{-2}$ eV.

VII. CONCLUSIONS

We have derived the post-Newtonian parameter and laboratory constraints on the spectral action with Standard Model content. The modified Newtonian potential (12) has its Yukawa amplitudes, with effective masses set by the particle content and the spectral scale Λ.

The central experimental result is:

$$\Lambda > 2.565 \times 10^{-3}\,\text{eV} \quad (95\%\ \text{CL, Eöt-Wash})\,,$$

corresponding to $1/\Lambda < 77\,\mu$m (Yukawa range $\lambda_1 < 36\,\mu$m). All solar-system tests are satisfied with exponential margin. Casimir, atom interferometry, and satellite experiments are below their sensitivity thresholds for the SCT coupling strengths.

The spectral action passes all currently available gravitational tests. The most promising avenue for future improvement is the extension of torsion-balance experiments to shorter ranges, which would directly constrain Λ in the meV regime.

ACKNOWLEDGMENTS

Numerical results were obtained using `mpmath` and `scipy` and verified to 100-digit precision.

AI DISCLOSURE

In preparing this manuscript, large language model tools (specifically Anthropic Claude Opus 4.7 and OpenAI ChatGPT GPT-5.5 Pro) were used for English-language editorial assistance, bibliographic cross-checking, LaTeX markup verification, and the writing of computational code and numerical-verification scripts that were subsequently audited by the author. All mathematical derivations, the choice of observables, the comparison against Cassini, lunar-laser-ranging, and short-range torsion-balance constraints, the figures, the interpretations, and the conclusions are the author's own. Every numerical value reported in the manuscript was computed by software written by the author (with AI assistance as declared) and was cross-checked against the canonical-validator modules of the upstream Spectral Causal Theory program at 100-digit precision. Every citation was individually verified against arXiv, Crossref, or the journal page of record. AI tools are not listed as authors and bear no authorial responsibility for this manuscript.

DATA AVAILABILITY

The computational tools and experimental data references used in this work are available from the author upon reasonable request.